Acta Cryst. (1995). B51, 746–753

A Composite Modulated Structure Refinement of $Zr_9(N,O,F)_{20}$

BY SIEGBERT SCHMID* AND RAY L. WITHERS

Research School of Chemistry, Australian National University, Canberra, ACT 0200, Australia

(*Received* 6 *September* 1994; *accepted* 9 *January* 1995)

Abstract

Single-crystal X-ray diffraction (Mo$K\alpha$ radiation) is used to determine the structure of $(Zr_9N_{8-z}F_{1-z}O_{2z})F_{11}$, a $\Delta = 0.22$ member of a wide-range non-stoichiometric solid solution in the zirconium nitride oxide fluoride system. The structure is refined as a compositely modulated structure composed of two mutually incommensurable Q and H substructures with overall superspace-group symmetry $Acmm(0,0,1.222..)0s0$. The $Zr_9N_{8-z}F_{1-z}O_{2z}$ subsystem has lattice parameters $a = 5.152(2)$, $b_Q = 5.364(2)$ and $c_Q = 5.379(2)$ Å, and substructure superspace-group symmetry $Acmm(0,0,1.222..)0s0$. The F subsystem has lattice parameters $a = 5.152(2)$, $b_H = \frac{1}{2}b_Q = 2.682(1)$ and $c_H = 4.401(2)$ Å, and substructure superspace-group symmetry $Pmcm(0,\frac{1}{2},0.8181...)s00$. Refinement on 460 unique reflections converged smoothly to $R = 0.019$.

1. Introduction

An anion-excess, fluorite-related solid solution occurs in the zirconium nitride fluoride/zirconium nitride oxide fluoride system (Jung & Juza, 1973; Schmid & Withers, 1994) for an anion-to-cation ratio between 2.12 and 2.25 (*i.e.* $MX_{2+\Delta}$, $0.12 \leq \Delta \leq 0.25$). Initially it was thought that this phase was a pure nitride fluoride. The formulation as a nitride oxide fluoride rather than a pure nitride fluoride is due to two recent papers by Schlichenmaier, Schweda, Strähle & Vogt (1993) and Schmid & Withers (1994), where it was found that the phase can contain a significant amount of oxygen (up to 10% of the total anion concentration).

To date, there has been only one single-crystal X-ray structure refinement within the composition range of the solid solution (Jung & Juza, 1973). This refinement was of $Zr_{108}N_{98}F_{138}$, corresponding to an anion-to-cation ratio of ~ 2.185, *i.e.* $\Delta = 0.185$. The resultant structure was described as a 27-fold superstructure of an anion-excess fluorite-related subcell. Although the positions of the weaker satellite reflections better approximated a 59-fold supercell, a 27-fold supercell was used in order to reduce the possible number of independent variables to be refined and also because the final R value for the latter (0.113) was only slightly higher.

Recently, it has been shown that the whole solid solution is best described as an incommensurate compositely modulated phase (Withers, Schmid & Thompson, 1993) composed of two substructures (Q and H), which are mutually commensurable along their a- and b-axis directions, but whose relative periodicity along their colinear c-axis directions is linearly dependent on the anion-to-cation ratio (Schmid & Withers, 1994). The strongly scattering Q substructure corresponds to the anion-excess fluorite-related subcell of Jung & Juza (1973), while the continuously variable composition-dependent primary modulation wavevector thereof, $\mathbf{q}_Q$, is given by a reciprocal lattice vector of the H substucture, *i.e.* $\mathbf{c}_H$*. In these terms, the 972 unique reflections Jung & Juza (1973) used for refinement of $Zr_{108}N_{98}F_{138}$ consisted of 240 parent, 414 first-order satellite, 58 second-order satellite, 252 third-order satellite and only 8 fourth-order satellite reflections. This has to be compared with the 27 orders of satellite reflections that should nominally be observable. The large number of unobserved satellite reflections causes special correlations between structural parameters which make the least-squares refinement of this structure in terms of a conventional superstructure difficult.

In general terms, all such structures can be described as inorganic misfit layer compounds characterized by a strictly alternate stacking of two different types of layers (Makovicky & Hyde, 1992). These two different types of layers can be described as a layer of pseudo-tetragonal edge-sharing $\{A\}M_4$ tetrahedra (consisting of a 4^4 net of anions sandwiched between similar but lower density nets of cations, *i.e.* a {100} layer of fluorite type) and a pseudo-hexagonal 3^6 net of anions. In accordance with IUCr convention, the first substructure is labelled Q and the second H (Guinier, 1984).

The general stoichiometry of the phase can be rewritten with respect to these two subsystems as $(ZrN_{1-\Delta/2-z}F_{\Delta/2-z}O_{2z})F_{1+\Delta}$, with $0.12 \leq \Delta \leq 0.25$. Note that there are as many anions in the Q substructure (the part of the formula in parentheses) as there are metal atoms, giving an overall Q substructure stoichiometry of ZrA. This means that the H substructure has to accommodate $1 + \Delta$ anions (where Δ is the number of additional anions with respect to the fluorite structure). Δ can be determined directly from the ratio of the average substructure c-axis dimensions c_Q/c_H. Measurement of average substructure unit-cell dimensions as a function of

* To whom correspondence should be addressed.

Table 1. *Important parameters for the data collection on* $(Zr_9N_{8-z}F_{1-z}O_{2z})F_{11}$

Space group	*Acmm* (0,0,1.222..)0s0
Cell dimensions	
a (Å)	5.152 (2)
b (Å)	5.364 (2)
c (Å)	48.411 (17)
c_Q (Å)	5.379 (2)
c_H (Å)	4.401 (2)
Formula weight	1061.01
Z	4
Density (g cm^{-3})	5.764
Wavelength (Å)	0.71069 (Mo $K\alpha$)
Monochromator	Graphite
Scan mode	ω scans
Scan width (° in ω)	$1.1 + 0.35\tan\theta$
Scan speed (° min^{-1})	1.5
Attenuation factor	16.04
μ (cm^{-1})	67.85
2θ range (°)	4–70
h, k, l range	±8, ±8, ±78
No. of collected reflections	23055
Unique reflections with $I > 3\sigma(I)$	460
No. of parameters	28
Absorption correction	Gaussian (14 × 14 × 14 grid)
Transmission factors	$0.646 \le T \le 0.718$
Extinction correction	Isotropic, type II, 0.044 (4)

Note: Composition-dependent parameters are calculated for $z = 0$ in the above formula.

composition shows that the variable stoichiometry is almost solely accommodated by variation in the H substructure c-axis dimension (Schmid & Withers, 1994). The exact stoichiometry, *i.e.* z in the above formula, is difficult to determine as substitutions of the type $2O^{2-} \Leftrightarrow N^{3-} + F^-$ may occur in the Q substucture without altering the overall anion-to-cation ratio and hence c_Q/c_H.

The symmetry of the composite system and of the two component subsystems has already been described in some detail (Withers, Schmid & Thompson, 1993; Schmid & Withers, 1994), however, the setting used in this paper is somewhat different (see §3). Following procedures described in a previous paper (Schmid & Withers, 1994), single crystals of a $\Delta = 0.22$ composition, *i.e.* $(Zr_9N_{8-z}F_{1-z}O_{2z})F_{11}$, within the above solid solution have been grown. The purpose of this paper is to present the results of a single-crystal X-ray structure refinement of these crystals using the superspace group approach.

2. Experimental

2.1. *Synthesis*

Single crystals of $(Zr_9N_{8-z}F_{1-z}O_{2z})F_{11}$ were grown according to procedures described previously (Jung & Juza, 1973; Schmid & Withers, 1994).

2.2. *Intensity measurement and data processing*

Preliminary investigations of the single crystal used for data collection gave the c axis ratio of the H and Q substructures as $\frac{9}{11}$, *i.e.* to within the accuracy of measurement, $\mathbf{c}_H^* = \frac{11}{9}\mathbf{c}_Q^*$. This enabled the data collection to be performed with respect to a 9 times **c** superstructure of the more strongly scattering Q substructure.

Accurate supercell-lattice parameters (see Table 1) were obtained from a least-squares fit of the setting angles for 25 reflections with 2θ values between 23 and 41° for Mo $K\alpha$ radiation. A Philips PW1100/20 diffractometer was used for data collection. Background counting time was 10 s on either side of the scan. Square slits subtended angles $1 \times 1°$ at the crystal. Lorentz–polarization and other subsequent corrections were performed using the program package *Xtal*3.0 (Hall & Stewart, 1990). The three standard reflections measured every 120 min showed a significant linear decrease in intensity of *ca* 30% throughout the 3 weeks of data collection time due to decreasing tube intensity. After correcting the data for this decrease in standard reflection intensities no unusual features were left. Averaging the reflection intensities in Laue symmetry *mmm* gave 460 unique reflections (internal $R = 0.036$ on F^2). Other important parameters for the data collection on $(Zr_9N_{8-z}F_{1-z}O_{2z})F_{11}$ are given in Table 1.†

3. Symmetry considerations

In a previous paper (Withers, Schmid & Thompson, 1993), the point-group symmetry of reciprocal space and the extinction conditions characteristic of all compositions within this solid solution were used to determine the overall superspace-group symmetry of this phase. Both underlying parent substructures ($a_Q = a_H$, $b_Q = 2b_H$, $c_Q \sim 1.2c_H$) as well as the analytical form of the atomic modulation functions (AMF's; Pérez-Mato, Madariaga, Zúñiga & Garcia Arribas, 1987) describing the mutual influence of the two parent substructures upon each other were also given. The primary modulation wavevectors characteristic of the Q and H substructures were given as $\mathbf{q}_Q = \mathbf{c}_H^* - 2\mathbf{c}_Q^*$ and $\mathbf{q}_H = \frac{1}{2}\mathbf{b}_H^* + \mathbf{c}_H^* - \mathbf{c}_Q^*$, respectively.

In this paper, following a recently suggested convention as regards the choice of primary modulation wavevectors for composite modulated structures (Yamamoto, 1992, 1993), all reflections are indexed with respect to a basis set of four reciprocal lattice vectors – namely $M^* = \{\mathbf{a}_Q^*, \mathbf{b}_Q^*, \mathbf{c}_Q^*, \mathbf{c}_H^*\}$. Similarly, following the convention originally proposed by de Wolff, Janssen & Janner (1981) and, more recently, by Janssen, Janner, Looijenga-Vos & de Wolff (1992), the unit cell of the H parent substructure given in Withers, Schmid & Thompson (1993; see Fig. 1 therein) has been doubled along the b direction so that the rational component of $\mathbf{q}_H$

† A list of structure factors has been deposited with the IUCr (Reference: JS0009). Copies may be obtained through The Managing Editor, International Union of Crystallography, 5 Abbey Square, Chester CH1 2HU, England.

Table 2. *Average substructure positions and anisotropic thermal parameters for the Q and H substructures*

Site	x	y	z	$U11$	$U22$	$U33$
$M1_Q$	−0.19225 (5)	1/4	0	0.0049 (1)	0.0045 (2)	0.0061 (1)
$A1_Q$	0	0	−1/4	0.007 (1)	0.0053 (9)	0.0064 (8)
$A1_H$	1/2	−0.1264 (4)	−1/4	0.008 (1)	0.0108 (8)	0.016 (1)

becomes an integer with respect to the above basis set. In this setting, $\mathbf{q}_Q = \mathbf{c}_H^*$ and $\mathbf{q}_H = \mathbf{c}_Q^*$.

With respect to this basis set, the reported extinction conditions (Withers, Schmid & Thompson, 1993) are now given by $F(HKLm) = 0$ unless $K + L = 2n$, $F(0KLm) = 0$ unless $K, L = 2n$ and $F(H0Lm) = 0$ unless $L, m = 2n$. The former condition requires a centring in superspace of the form $\{E|0, \frac{1}{2}, \frac{1}{2}, 0\}$, the next a glide plane $\{\sigma_x|0, \frac{1}{2}, 0, 0\}$ and the latter a glide plane of the form $\{\sigma_y|0, \frac{1}{2}, 0, \frac{1}{2}\}$. In conjunction with the *mmm* point-group symmetry of reciprocal space, the implied superspace group is *Acmm*(0,0,1.222..)0*s*0 in the notation of Janssen, Janner, Looijenga-Vos & de Wolff (1992). The generators of both the Q and H component substructure-superspace groups (van Smaalen, 1991) can now be derived by the use of the appropriate permutation matrices [$W^Q = P^Q = (1)$ and $W^H = P^H = (3, 4)$ in the notation of Yamamoto (1993)] and are given by $\{E|0, \frac{1}{2}, \frac{1}{2}, 0\}_Q$, $\{\sigma_x|0, \frac{1}{2}, 0, 0\}_Q$, $\{\sigma_y|0, \frac{1}{2}, 0, \frac{1}{2}\}_Q$ and $\{i|000, 2\delta\}_Q$ in the case of the Q substructure and $\{E|0, \frac{1}{2}, 0, \frac{1}{2}\}_H$, $\{\sigma_x|0, \frac{1}{2}, 0, 0\}_H$, $\{\sigma_y|0, \frac{1}{2}, \frac{1}{2}, 0\}_H$ and $\{i|00, 2\delta, 0\}_H$ in the case of the H substructure. The corresponding Q substructure component superspace group is *Acmm*(0,0,1.222..)0*s*0. The corresponding H substructure component superspace group (with respect to the true H substructure unit-cell dimensions of a, b_H, c_H) is *Pmcm*$(0, \frac{1}{2}, 0.8181...)s00$.

The relative origin of the two substructures has been fixed by application of the superspace-group symmetry operation $\{i|000, 2\delta\}$ to the entire composite structure. In terms of the expressions for the AMF's derived in the previous paper (Withers, Schmid & Thompson, 1993), this corresponds to putting $\theta(\mathbf{q}_Q) = 180° - 2\pi\mathbf{c}_H^*.\frac{1}{4}\mathbf{c}_Q - 2\pi\delta$ and $\theta(\mathbf{q}_H) = 0° + 2\pi\mathbf{c}_Q^*.\delta\mathbf{c}_H$, respectively. As a consequence, the two substructures have a common origin at $\frac{1}{4}\mathbf{c}_Q$ and $(\frac{1}{4} - \delta)\mathbf{c}_H$, respectively, with respect to the origins shown in Fig. 1 of Withers, Schmid & Thompson (1993), *i.e.* the $M1$ or Żr (site symmetry 2*mm*) and $A1$ or (N,O,F) (site symmetry 222) sites of the average Q substructure now occur with fractional coordinates given by $x, \frac{1}{4}, 0$ and $0, 0, -\frac{1}{4}$, respectively (with $x \sim -0.19$), while the $A1$ or F (site symmetry *m*2*m*) site of the average H substructure now occurs with fractional coordinates given by $\frac{1}{2}, y, (\delta - \frac{1}{4})$ with $y \sim -\frac{1}{8}$ ($\sim -\frac{1}{8}$ rather than $\sim -\frac{1}{4}$ as a result of the doubled $\mathbf{b}_H$ axis; see Table 2).

The constraints on the allowed displacements associated with even- and odd-order modulation waves are as given previously (Withers, Schmid & Thompson, 1993). With respect to the above origin, the displacive AMF's describing the structural deviation of the $M1$ and $A1$ atoms away from their positions in the average Q substructure are given by

$$\begin{aligned} U_{M1}(\mathbf{T}_Q) = \mathbf{a}_Q &\sum_{2n=2,4,\ldots} \varepsilon_{Mx}(2n\mathbf{q}_Q)\cos(2n2\pi[\mathbf{q}_Q.\mathbf{T}_Q - \delta]) \\ &- \mathbf{b}_Q \sum_{2n+1=1,3,\ldots} \varepsilon_{My}((2n+1)\mathbf{q}_Q) \\ &\times \sin((2n+1)2\pi[\mathbf{q}_Q.\mathbf{T}_Q - \delta]) \\ &- \mathbf{c}_Q \sum_{2n=2,4,\ldots} \varepsilon_{Mz}(2n\mathbf{q}_Q)\sin(2n2\pi[\mathbf{q}_Q.\mathbf{T}_Q - \delta]) \end{aligned}$$

$$\begin{aligned} U_{A1}(\mathbf{T}_Q) = -\mathbf{a}_Q &\sum_{2n+1=1,3,\ldots} \varepsilon_{Ax}((2n+1)\mathbf{q}_Q) \\ &\times \cos((2n+1)2\pi[\mathbf{q}_Q.(\mathbf{T}_Q - \tfrac{1}{4}\mathbf{c}_Q) - \delta]) \\ &+ \mathbf{b}_Q \sum_{2n+1=1,3,\ldots} \varepsilon_{Ay}((2n+1)\mathbf{q}_Q) \\ &\times \sin((2n+1)2\pi[\mathbf{q}_Q.(\mathbf{T}_Q - \tfrac{1}{4}\mathbf{c}_Q) - \delta]) \\ &- \mathbf{c}_Q \sum_{2n=2,4,\ldots} \varepsilon_{Az}(2n\mathbf{q}_Q) \\ &\times \sin(2n2\pi[\mathbf{q}_Q.(\mathbf{T}_Q - \tfrac{1}{4}\mathbf{c}_Q) - \delta]), \end{aligned}$$

where $\mathbf{q}_Q = \mathbf{c}_H^*$, $\mathbf{T}_Q$ is a Bravais lattice vector of the Q substructure and $n = m_Q$ is an integer which labels the harmonic order of the corresponding modulation wave with respect to the underlying Q substructure. The corresponding displacive AMF's describing the structural deviation of the $A1$ atoms away from their positions in the average H substructure are given by

$$\begin{aligned} U_{A1}(\mathbf{T}_H) = \mathbf{a}_H &\sum_{2n+1=1,3,\ldots} \varepsilon_{Ax}((2n+1)\mathbf{q}_H)\cos(n\pi \\ &+ (2n+1)2\pi[\mathbf{q}_H.(\mathbf{T}_H + [\delta - \tfrac{1}{4}]\mathbf{c}_H) + \mathbf{b}_Q^*.\mathbf{T}_H]) \\ &+ \mathbf{b}_H \sum_{2n=2,4,\ldots} \varepsilon_{Ay}(2n\mathbf{q}_H)\cos(n\pi \\ &+ 2n2\pi[\mathbf{q}_H.(\mathbf{T}_H + [\delta - \tfrac{1}{4}]\mathbf{c}_H) + \mathbf{b}_Q^*.\mathbf{T}_H]) \\ &+ \mathbf{c}_H \sum_{2n=2,4,\ldots} \varepsilon_{Az}(2n\mathbf{q}_H)\sin(n\pi + 2n2\pi \\ &\times [\mathbf{q}_H.(\mathbf{T}_H + [\delta - \tfrac{1}{4}]\mathbf{c}_H) + \mathbf{b}_Q^*.\mathbf{T}_H]), \end{aligned}$$

where $\mathbf{q}_H = \mathbf{c}_Q^*$, $\mathbf{T}_H$ is a Bravais lattice vector of the H substructure (including the translation $\mathbf{b}_H = \frac{1}{2}\mathbf{b}_Q$) and $n = m_H$ is an integer which labels the harmonic order of the corresponding modulation wave with respect to the underlying H substructure. The refined values for these displacive modulation wave amplitudes (see Table 3) can be compared directly with those recently obtained from a Fourier decomposition of the reported crystal structure of $Zr_{108}N_{98}F_{138}$ (Withers, Schmid & Thompson, 1993).

4. Refinement details

The refinements were carried out using the software package *JANA*94 (Petrícek, 1994). The atomic scattering factors are from *International Tables for X-ray Crystal-*

Table 3. *Modulation wave amplitudes for the structure refinement of* $Zr_9(N,O,F)_{20}$ (*a*) *Q and* (*b*) *H substructure*; *note*: '0' *denotes* 0 *by symmetry*

(*a*)

n	$\varepsilon_{Mx}(n\mathbf{q}_Q)$	$\varepsilon_{My}(n\mathbf{q}_Q)$	$\varepsilon_{Mz}(n\mathbf{q}_Q)$
1	0	−0.03283 (8)	0
2	−0.00051 (18)	0	−0.00268 (13)
3	0	−0.01129 (10)	0
n	$\varepsilon_{Ax}(n\mathbf{q}_Q)$	$\varepsilon_{Ay}(n\mathbf{q}_Q)$	$\varepsilon_{Az}(n\mathbf{q}_Q)$
1	0.04582 (72)	−0.02612 (70)	0
2	0	0	−0.00106 (123)
3	−0.00530 (152)	0.01155 (85)	0

(*b*)

n	$\varepsilon_{Ax}(n\mathbf{q}_H)$	$\varepsilon_{Ay}(n\mathbf{q}_H)$	$\varepsilon_{Az}(n\mathbf{q}_H)$
1	0.07934 (60)	0	0
2	0	−0.00171 (62)	−0.00239 (90)
3	0.00979 (76)	0	0
4	0	−0.00196 (71)	0.00382 (90)

lography (Vol. IV, 1974). The structure was initially refined as a commensurate composite structure with the parameter δ chosen as zero corresponding to a three-dimensional supercell space-group symmetry of *Pbcb*. Note that the possible three-dimensional supercell space-group symmetries of $(Zr_9N_{8-z}F_{1-z}O_{2z})F_{11}$, where c_H/c_Q apparently equals 9/11 exactly, can be derived from the superspace-group symmetry given in §3 (see Yamamoto & Nakazawa, 1982; Wiegers *et al.*, 1990) and are given by

$$Pbcb \text{ (for } \delta = 2N/36, N \text{ an integer)}$$

$$Pbcm \text{ (for } \delta = (2N+1)/36)$$

$$Pbc2_1 \text{ (otherwise).}$$

The starting model for the refinement of the structure (*i.e.* starting values for the above displacive modulation wave amplitudes) was taken from the Fourier decomposition of the published structure of $Zr_{108}N_{98}F_{138}$ (Withers, Schmid & Thompson, 1993). In the first step only the average substructures were refined using both sets of parent reflections. The major displacive modulation wave amplitude for each of the atoms, *i.e.* $\varepsilon_{My}(\mathbf{q}_Q)$, $\varepsilon_{Ax}(\mathbf{q}_Q)$ and $\varepsilon_{Ax}(\mathbf{q}_H)$ was then added and refined starting with the value as derived from $Zr_{108}N_{98}F_{138}$ and using parent and first-order satellite reflections of both substructures. All possible sign combinations for these modulation wave amplitudes were tested in the refinement. The correct combination of signs resulted in significantly lower *R*-values than any of the other possibilities. The remaining modulation wave amplitudes were then released for refinement with zero as starting values. False minima were investigated by systematically reversing the sign of various modulation wave amplitudes. In each case, the refinement self-corrected, *i.e.* the corresponding amplitudes in each case reversed sign to return to their original values.

The lack of observed higher-order satellite reflections [no satellite reflections of order higher than $n = 4$, $n = \min(|m_Q|, |m_H|)$, were observed] suggested, however, that the relative origin of the two substructures, *i.e.* δ, might well be an unrefineable parameter (see, for example, Pérez-Mato, 1991). Hence, the structure was also refined as an incommensurate composite structure (see, for example, Yamamoto, 1993). Refinement as an incommensurate structure entails an integration over all possible relative origins of the two substructures.

Table 4. *Refinement statistics* (%)

n	No. of reflections	Model 1	Model 2
0	212	1.49	1.50
1	206	2.10	2.10
2	11	8.52	8.43
3	29	5.81	5.79
4	2	17.22	17.20
R_{all}	460	1.87	1.87
R_w	460	2.63	2.62

Model 1: incommensurate refinement; model 2: commensurate refinement.

This refinement as an incommensurate structure led to almost identical *R*-values and converged smoothly to a final overall *R*-value of 0.019 once an isotropic extinction correction had been incorporated (see Table 4). Refinement using full-matrix least squares was on *F*. An additional uncorrelated error of 0.01 was included with the counting statistic estimate in the evaluation of weights. Atoms were refined with anisotropic thermal parameters. The anion positions in the *Q* substructure were occupied with 8/9N+1/9F. The final refined parameters for the average substructures are given in Table 2 and the final refined displacive modulation wave amplitudes in Table 3. All major modulation wave amplitudes agree very well with the values derived from the structure of $Zr_{108}N_{98}F_{138}$, as is evident from a comparison of the displacive modulation wave amplitudes listed in Table 3 and those given in Tables 1 and 2 of Withers, Schmid & Thompson (1993). The refinement statistics for the incommensurate model (Model 1) and the commensurate *Pbcb* model (Model 2) split into reflection classes labelled by the harmonic order of the reflections are given in Table 4 (note: refinements as a commensurate structure were also carried out at values of δ other than zero, but gave identical refinement statistics and are not reported here).

5. Results and discussion

5.1. *Atomic modulation functions*

The refined displacive atomic modulation functions (AMF's) for the final model, *i.e.* $\mathbf{U}_{M1}$ as a function of $(\mathbf{q}_Q\cdot\mathbf{T}_Q - \delta)$ modulo an integer and $\mathbf{U}_{A1}$ as a function of $[\mathbf{q}_Q\cdot(\mathbf{T}_Q - \frac{1}{4}\mathbf{c}_Q) - \delta]$ modulo an integer for the *Q* substructure, as well as $\mathbf{U}_{A1}$ as a function of $\mathbf{q}_H\cdot(\mathbf{T}_H + [\delta - \frac{1}{4}]\mathbf{c}_H)$ modulo an integer for the *H* substructure, are shown in Figs. 1–3, respectively. Note that Zr occupies the *M*1 site and (N,O,F) the *A*1 site of the *Q* substructure, while the *A*1 site of the *H* substructure is occupied by F alone. The Zr atoms of

the Q substructure show a large modulation amplitude only along the b direction, whereas the anions of the Q substructure are strongly modulated along both a and b directions. The F atoms of the H substructure show strong modulation only along the a direction. None of the atoms display a significant modulation amplitude along **c**.

Fig. 4 shows the variation in the coordination sphere of Zr as a function of $(\mathbf{q}_Q \cdot \mathbf{T}_Q - \delta)$ modulo an integer. Each Zr atom is coordinated by four N (O, F) atoms within the same substructure. The distances between the Zr atoms and these anions in the Q substructure (the dot–dashed lines) do not show a large variation, although a

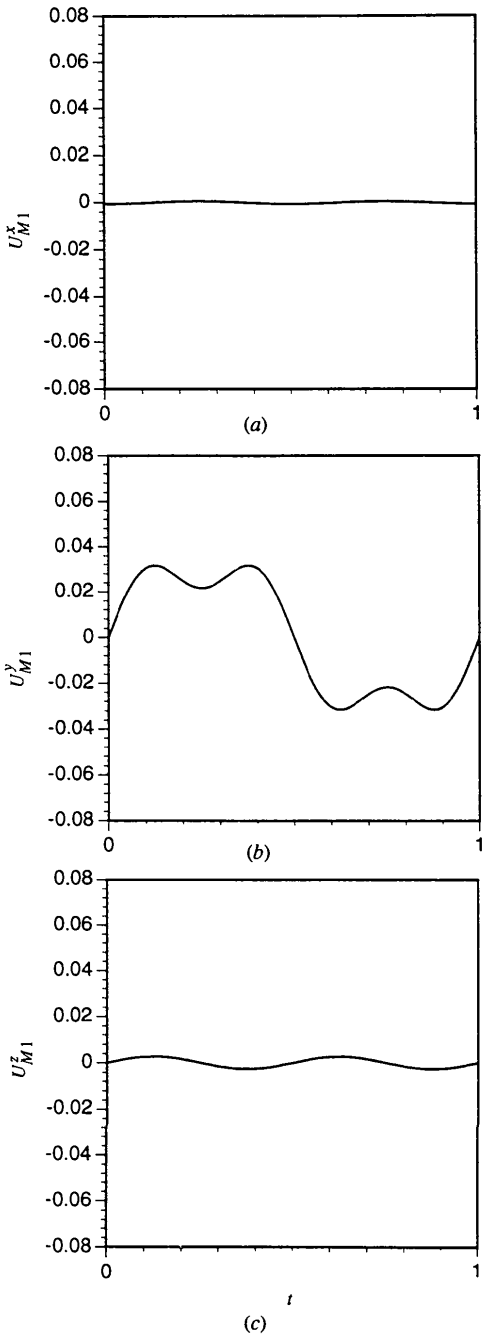

Fig. 1. Final refined Q substructure metal atom AMF's, *i.e.* (*a*) U^x_{M1}, (*b*) U^y_{M1} and (*c*) U^z_{M1} plotted in fractional coordinates as a function of $t = (\mathbf{q}_Q \cdot \mathbf{T}_Q - \delta)$ modulo an integer.

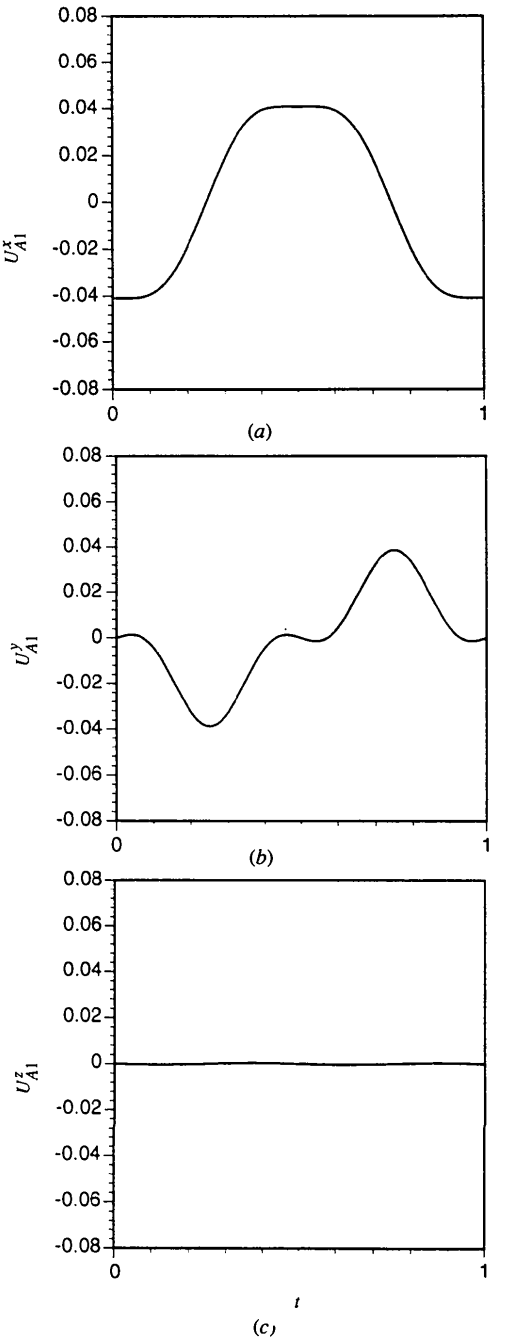

Fig. 2. Final refined Q substructure anion AMF's, *i.e.* (*a*) U^x_{A1}, (*b*) U^y_{A1} and (*c*) U^z_{A1} plotted in fractional coordinates as a function of $t = [\mathbf{q}_Q \cdot (\mathbf{T}_Q - \frac{1}{4}\mathbf{c}_Q) - \delta]$ modulo an integer.

difference of ~ 0.16 Å between minimum and maximum values is certainly significant. The distances between Zr and the F atoms in the *H* substructure (the solid lines) show a larger variation (note: in the incommensurate case this range is given by the minimum distance and infinity) due to the fact that the two substructures literally shift past each other, resulting in a continuously changing coordination sphere. This distance variation leads to overall metal coordination ranging from 6 to 8 with clearly quite irregular coordination polyhedra.

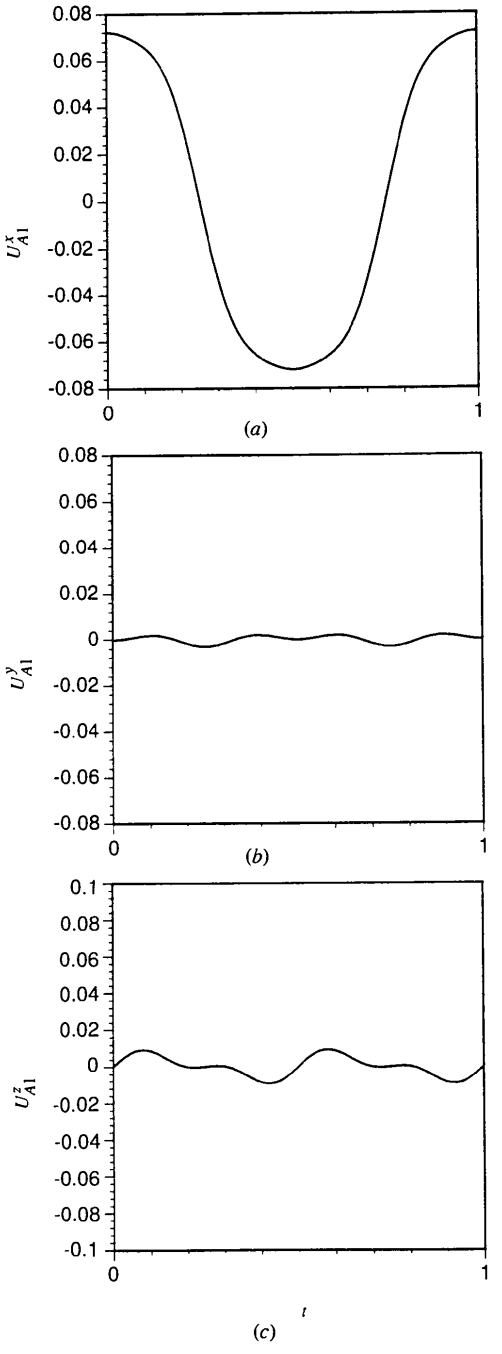

Fig. 3. Final refined *H* substructure anion AMF's, *i.e.* (*a*) U^x_{A1}, (*b*) U^y_{A1} and (*c*) U^z_{A1} plotted in fractional coordinates as a function of $t = \mathbf{q}_H \cdot (\mathbf{T}_H + [\delta - \frac{1}{4}]\mathbf{c}_H)$ modulo an integer.

Fig. 5 shows a projection of the structure down **b**. One 'supercell' along **c** ($\mathbf{c} = 9\mathbf{c}_Q = 11\mathbf{c}_H$) is shown. Unit cells of both parent substructures are outlined (common origin at the bottom left corner). This origin corresponds to $\delta = 0$ resulting in a 'supercell' space-group symmetry of *Pbcb*. It is readily seen that the F atoms move strongly along the *a*, *i.e.* layer stacking, direction. The anions in the *Q* substructure also move along the *a* direction although to a lesser extent. The metals, however, do not move at all along **a** (*cf.* the appropriate AMF's). None of the atoms show any significant motion along **c**. The projection down **a** in Fig. 6 shows that the *H* substructure is virtually undistorted along both **b** and **c**, whereas the metal atoms and anions of the *Q* substructure move significantly along **b** but not along **c**. Fig. 6 shows that the *H* substructure is an almost perfect 3^6-net in projection along **a**. This 3^6-net, however, is substantially buckled as can be seen from the large amplitude motion along **a** shown in Fig. 5. Similarly, while the anions in the 4^4-net appear to remain in the centre of the surrounding tetrahedron of metal atoms in projection down **a**, it can be seen in Fig. 5 that they do move significantly off the centre of the tetrahedra along **a**.

5.2. *Apparent valence calculations*

Apparent valences (AV's; Brown & Altermatt, 1985; O'Keeffe, 1989) are often an extremely useful guide to the reliability of refined crystal structures and have previously been calculated for a number of structures that belong to the same type of inorganic misfit layer compounds, *e.g.* $Zr_{108}N_{98}F_{138}$, $Y_7O_6F_9$ (Schmid & Withers, 1994). For $Zr_{108}N_{98}F_{138}$, it was found that the N and Zr atoms ended up with AV's that suggested

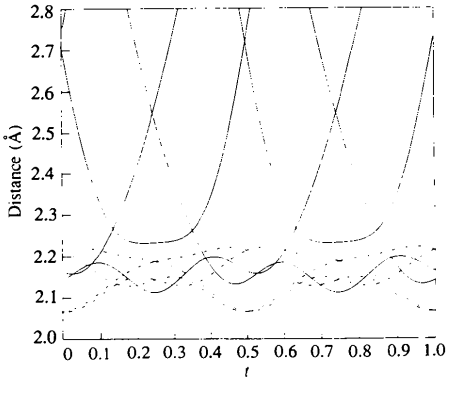

Fig. 4. Shows the variation in the coordination sphere of Zr as a function of $t = (\mathbf{q}_Q \cdot \mathbf{T}_Q - \delta)$ modulo an integer. The distances between the Zr's and the anions in the *Q* substructure are shown by the dot–dashed lines, whereas the distances between Zr and F atoms in the *H* substructure are shown by the solid lines.

strong overbonding, while the spread of the values (±0.2 units) was assumed to be within error.

In order to calculate AV's for $(Zr_9N_{8-z}F_{1-z}O_{2z})F_{11}$, atomic coordinates in a supercell approximation were derived from the AMF's given above, assuming $\delta = 0$. The conventional three-dimensional space-group with this origin is *Pbcb*, a non-standard setting of *Pcca* (No. 54). There are then five crystallographically independent Zr and anion positions in the *Q* substructure and six F positions in the *H* substructure. The corresponding AV's [r_0^{ij}: $(Zr^{4+}—N^{3-}) = 2.11$ Å; $(Zr^{4+}—F^{-}) = 1.854$ Å; *EUTAX* (Brese & O'Keeffe, 1991)] range from 4.4 to 4.5 for the Zr atoms, 3.3–3.4 for the *Q* substructure anions and 0.9–1.0 for the *H* substructure anion sites (note: AV's calculated with *Q* substructure anion sites occupied by $\frac{8}{9}$N and $\frac{1}{9}$F). These AV's do not substantially differ from the values calculated for $Zr_{108}N_{98}F_{138}$ (Schmid & Withers, 1994). In particular, the N and Zr atoms again ended up with AV's indicating strong overbonding. Given the quality of the present refinement of $(Zr_9N_{8-z}F_{1-z}O_{2z})F_{11}$, one would expect to obtain reasonable AV's.

Two possible reasons for such a deviation from the expected values could be that the positions of the N atoms are not correct or that the bond-length/bond-valence parameter $r_0^{ij}(Zr^{4+}—N^{3-})$ is not determined accurately enough (Brese & O'Keeffe, 1991). A recent review of inorganic nitrides (Brese & O'Keeffe, 1992) gives only very few examples of zirconium nitrides, suggesting that the listed r_0^{ij} parameter for $Zr^{4+}—N^{3-}$ is based on very few experimental refinements. Therefore, it might well be that $r_0^{ij}(Zr^{4+}—N^{3-})$ is not the value that should be used for our particular structure. As the parameters of the *Q* substructure are refined with low standard deviations it is considered less likely that the mentioned deviations in AV's result from inaccurate coordinates.

The apparent overbonding of the *Q* substructure anions could be reduced by fixing them at the centre of their surrounding metal tetrahedra. The refinement, however, shows that these anions clearly do move from the centre of their surrounding metal tetrahedra. Such motion is similar to the corresponding motion of O atoms in isostructural Y—O—F compounds (Bevan, Mohyla, Hoskins & Steen, 1990). In these latter cases, the *Q* substructure anions (and metals) show no indication of overbonding (Schmid & Withers, 1994). In summary, it would appear that the bond valence parameter, r_0^{ij}, for $Zr^{4+}—N^{3-}$ needs to be modified for this type of structure.

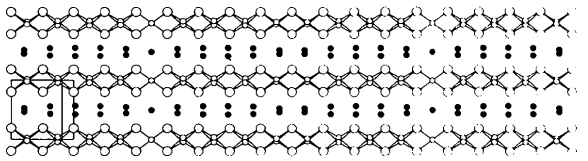

Fig. 5. A projection of the structure down **b**. One 'supercell' along **c** ($\mathbf{c} = 9\mathbf{c}_Q = 11\mathbf{c}_H$) is shown. The unit cells of both parent substructures are outlined (common origin at the bottom left corner). **a** up the page, **c** to the right. *Q* substructure atoms are shown as open circles (Zr large; *A* small) and *H* substructure atoms as full circles.

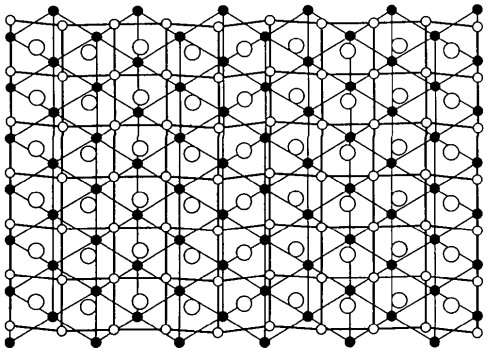

Fig. 6. A projection of part of the structure down **a**, **b** up the page, **c** to the right. *Q* substructure atoms are shown as open circles (Zr large; *A* small) and *H* substructure atoms as full circles.

6. Concluding remarks

A composite modulated structure approach has been used to refine and describe the structure of $(Zr_9N_{8-z}F_{1-z}O_{2z})F_{11}$. Starting values for the displacive modulation wave amplitudes used in the refinement were derived from a previously reported structure refinement of a single crystal with different composition. If regarded as conventional three-dimensional structures, these structures would appear to be quite different – they would have to be described by different space groups for example. Refinement in terms of modulation waves, however, reveals the extraordinary similarity of the structures – both being members of the same solid solution. The pattern of atomic displacements expressed by the AMF's and presented in this paper can, therefore, be taken as being representative of the whole solid solution. The similarity between commensurate and incommensurate refinements, given the continuously variable primary modulation wavevector (Schmid & Withers, 1994), shows that the structure is best described as an incommensurate composite structure.

The authors wish to thank Dr A. Yamamoto for his programs *MODPLT* used for plotting Fig. 4 and *PRJMS* used for plotting Figs. 5 and 6.

References

BEVAN, D. J. M., MOHYLA, J., HOSKINS, B. F. & STEEN, R. J. (1990). *Eur. J. Solid State Inorg. Chem.* **27**, 451–465.
BRESE, N. E. & O'KEEFE, M. (1991). *Acta Cryst.* B**47**, 192–197.
BRESE, N. E. & O'KEEFE, M. (1992). *Struct. Bonding*, **79**, 307–378.
BROWN, I. D. & ALTERMATT, D. (1985). *Acta Cryst.* B**41**, 244–247.
GUINIER, A. (1984). *Acta Cryst.* A**40**, 399–404.

HALL, S. R. & STEWART, J. M. (1990). Editors. *Xtal3.0 Reference Manual*. Univs. of Western Australia, Australia, and Maryland, USA.
JANSSEN, T., JANNER, A., LOOIJENGA-VOS, A. & DE WOLFF, P. M. (1992). *International Tables for Crystallography*, edited by A. J. WILSON, Vol. C, pp. 797–835. Dordrecht: Kluwer Academic Publishers.
JUNG, W. & JUZA, R. (1973). *Z. Anorg. Allg. Chem.* **399**, 129–147.
MAKOVICKY, E. & HYDE, B. G. (1992). *Non-Commensurate Layered Structures*, edited by A. MEERSCHAUT, pp. 1–100. Trans Tech Publications.
O'KEEFE, M. (1989). *Struct. Bonding*, **71**, 161–190.
PÉREZ-MATO, J. M. (1991). *Methods of Structural Analysis of Modulated Structures and Quasi-Crystals*, edited by J. M. PÉREZ-MATO, F. J. ZÚÑIGA & G. MADARIAGA, pp. 117–128. Singapore: World Scientific.
PÉREZ-MATO, J. M., MADARIAGA, G., ZÚÑIGA, F. J. & GARCIA ARRIBAS, A. (1987). *Acta Cryst.* A**43**, 216–226.
PETRÍCEK, V. (1994). *Programs for Modulated and Composite Crystals*. Institute of Physics, Praha, Czech Republic.
SCHLICHENMAIER, R., SCHWEDA, E., STRÄHLE, J. & VOGT, T. (1993). *Z. Anorg. Allg. Chem.* **619**, 367–373.
SCHMID, S. & WITHERS, R. L. (1994). *J. Solid State Chem.* **109**, 391–400.
SMAALEN, S. VAN (1991). *Phys. Rev. B*, **43**, 11330–11341.
WIEGERS, G. A., MEETSMA, A., HAANGE, R. J., VAN SMAALEN, S., DE BOER, J. L., MEERSCHAUT, A., RABU, P. & ROUXEL, J. (1990). *Acta Cryst.* B**46**, 324–332.
WITHERS, R. L., SCHMID, S. & THOMPSON, J. G. (1993). *Acta Cryst.* B**49**, 941–951.
WOLFF, P. M. DE, JANSSEN, T. & JANNER, A. (1981). *Acta Cryst.* A**37**, 625–636.
YAMAMOTO, A. (1992). *Acta Cryst.* A**48**, 476-483.
YAMAMOTO, A. (1993). *Acta Cryst.* A**49**, 831–846.
YAMAMOTO, A. & NAKAZAWA, H. (1982). *Acta Cryst.* A**38**, 79–86.

Acta Cryst. (1995). B**51**, 753–757

Isosymmetric Structural Phase Transitions: Phenomenology and Examples

BY ANDREW G. CHRISTY

Research School of Chemistry, The Australian National University, Canberra, ACT 0200, *Australia*

(*Received* 26 *September* 1994; *accepted* 6 *February* 1995)

Abstract

Structural phase transitions ('type 0') in which there is no change of space group or of the occupied Wyckoff sites contrast with others in which diffusionless transformation can occur in a single step between higher- and lower-symmetry space groups (type I), through a low-symmetry transition state between relatively higher-symmetry initial and final structures (type II), and those where the mechanism is necessarily more complex (type III). A phenomenological model shows that type 0 transitions are necessarily first order, and may terminate at a critical point. The corresponding supercritical behaviour is a 'crossover' or 'diffuse transition' in which there is no discontinuity in any free-energy derivative. However, the location of the crossover is precisely defined at a minimum in the second derivative of the free energy with respect to a suitable order parameter. Isosymmetric transitions and/or crossovers occur in important mineralogical systems (pyroxenes, feldspars and carbonates) and non-linear optic materials ($KTiOPO_4$). Non-monotonic variation of free-energy derivatives around the crossover can have a serious effect on the locations and slopes of phase equilibria in pressure–temperature space. Interaction between non-symmetry-breaking and symmetry-breaking order parameters appears to play a major rôle in stabilizing low-symmetry clinopyroxene and anorthite feldspar phases.

1. Introduction

This paper presents an extension of an approach to the classification of phase transitions that has been outlined previously (Christy, 1993). In that work, three types of transition were rigorously distinguished on symmetry criteria:

(1) Transitions in which a low-symmetry (LS) phase is obtained from a high-symmetry (HS) phase by atomic displacements which are consistent with a unique non-identity irreducible representation of the higher symmetry. These type I transitions can be modelled phenomenologically using Landau theory, and can be first or second order thermodynamically.

(2) 'Type II' transitions in which two different HS structures share a common LS phase and can be regarded as having special cases of the LS structure which arise when a structural parameter of the LS structure takes special values. The initial and final structures (HS) and transition state (LS) of a 'martensitic' transition are examples. The free energy of such systems may be expressed as a Fourier series in the appropriate order parameter. Examples are reviewed in Tolédano & Dmitriev (1993) and described in more detail in papers cited therein.

(3) 'Type III' transitions, where the atomic rearrangements involved are more complex. These can be decomposed into multiple type I and type II steps, which link various transition states of specific symmetry.